2nd URSI AT-RASC, Gran Canaria, 28 May – 1 June 2018

In-situ Verification of Aperture-Array Polarimetric Performance by means of a Micro UAV: Preliminary Results on the LOFAR Low Band Antenna

Fabio Paonessa[(1)], Giuseppe Virone[(1)], Stefania Matteoli[(1)], Pietro Bolli[(2)], Giuseppe Pupillo[(3)], Stefan J. Wijnholds[(4)], Andrea M. Lingua[(5)], Giuseppe Addamo[(1)], Oscar A. Peverini[(1)]
(1) Istituto di Elettronica e di Ingegneria dell'Informazione e delle Telecomunicazioni, CNR, Turin, Italy
(2) Osservatorio Astrofisico di Arcetri, INAF, Florence, Italy
(3) Istituto di Radioastronomia, INAF, Bologna, Italy
(4) Netherlands Institute for Radio Astronomy, Dwingeloo, The Netherlands
(5) Department of Environment, Land and Infrastructure Engineering, Polytechnic of Turin, Turin, Italy

Abstract

In order to assess the polarimetric performance of phased arrays for radio astronomy, the Intrinsic Cross-polarization Ratio (IXR) can be adopted as a figure of merit. An innovative technique employing an Unmanned Aerial Vehicle (UAV) to measure the IXR of low-frequency instruments (VHF/UHF bands) has been recently exploited on a station of the Low Frequency Array (LOFAR) radio telescope. We present results from a spin flight measurement demonstrating 35 dB IXR in boresight, a value close to the performance limits of the current measurement system.

1. Introduction

Many scientific aims for modern radio astronomy require the measurement of the polarization state of radio signals emitted by celestial sources. The Intrinsic Cross-polarization Ratio (IXR) [1] estimates the orthogonality between the output channels of a polarimeter independently of the chosen coordinate system. For this reason, such figure of merit can be effectively adopted to assess the polarimetric performance of radio astronomical phased arrays [2]-[6].
The IXR of a dual-polarized antenna system can be computed from the two complex-valued feed radiation patterns. In the case of low-frequency arrays for radio astronomy, such as the Low Frequency Aperture Array (LFAA) of the Square Kilometer Array (SKA) [7] and its precursors, the experimental determination of phase patterns is not straightforward. In [8], an innovative procedure to characterize the IXR without the knowledge of the absolute phase patterns has been described. It employs a linearly-polarized flying test source mounted on an Unmanned Aerial Vehicle (UAV) [9] to excite the antennas with several polarization angles (spin flights). This tool (see Fig. 1) was already used for the characterization of the amplitude radiation pattern of single elements, embedded elements and arrays based on various antenna configurations [10]-[13].

Figure 1. Partial view of the LOFAR array with the UAV flying above it.

This paper presents an experimental result in which the UAV-based technique has been applied to the Low Frequency Array (LOFAR) radio telescope [14].

2. Measurement technique

The output of a polarimeter in response to an incoming plane wave (far-field) can be described by its Jones matrix

$$\begin{bmatrix} v_a \\ v_b \end{bmatrix} = \begin{bmatrix} J_{a\hat{u}} & J_{a\hat{v}} \\ J_{b\hat{u}} & J_{b\hat{v}} \end{bmatrix} \begin{bmatrix} E_{\hat{u}}^{inc} \\ E_{\hat{v}}^{inc} \end{bmatrix}, \quad (1).$$

where v_a and v_b are the voltages measured at the output of the two polarimeter channels a and b, respectively, whereas $E_{\hat{u}}^{inc}$ and $E_{\hat{v}}^{inc}$ represent the two field components of the incoming plane wave. It should be noted that all the terms in (1) depend on the observation direction (ϑ, φ), which is understood for conciseness.
According to the relation (18) in [1], the IXR can be directly computed from the condition number of the Jones matrix $k(J)$. Moreover, it can be also shown that the Jones

matrix can be fully determined from the two complex radiation patterns of the polarimeter antennas a and b.
In [8], a convenient representation of the Jones matrix has been proposed in order to identify the pattern parameters involved in the IXR calculus and provide some physical interpretations. The relationship (4) in [8], hereby reproduced for convenience,

$$J \propto \begin{bmatrix} 1 & 0 \\ 0 & e^{j\varphi_{ab}} \end{bmatrix} \begin{bmatrix} 1 & 0 \\ 0 & m_{ab} \end{bmatrix} \begin{bmatrix} \cos(\delta_a) & \sin(\delta_a)e^{j\varphi_a} \\ -\sin(\delta_b)e^{j\varphi_b} & \cos(\delta_b) \end{bmatrix}, \quad (2).$$

allows to represent the Jones matrix by means of the following parameters. m_{ab} and φ_{ab} represent the magnitude and the phase, respectively, of the complex ratio between the radiation pattern of the two polarizations a and b; whereas the angles δ_a, φ_a, δ_b and φ_b parametrize the two polarization unit-vectors (i.e. the normalized field components). From (2), it should be noted that the parameter φ_{ab} does not affect the condition number of the Jones matrix $k(J)$.
This parametrization can be represented with the Poincaré sphere, as shown for a single polarization in Fig. 2, where τ and ε are the tilt and ellipticity of the corresponding polarization ellipse. Each colored circle represents the polarization states than can be achieved within a 180° variation of φ and with a constant value of $|\delta|$. For example, the blue circle is obtained for $|\delta| = 45°$, whereas the cyan is obtained for $|\delta| = 15°$. The equatorial plane in Fig. 2 ($\varepsilon = 0$) corresponds to all the linear polarization states whereas the north and south poles represent the two circular polarization states. The parametrization is complete because all the possible polarization states can be represented.
As described in [8], the experimental evaluation of the aforementioned parameters, which in turn allow to compute the IXR, is performed using a flying linearly-polarized field source which can rotate around the vertical axis (variable bearing angle, i.e. heading). The known quantities $E_{\hat{u}}^{inc}$ and $E_{\hat{v}}^{inc}$ depend on the scan strategy. For example, for a spin flight at zenith,

$$\begin{aligned} E_{\hat{u}}^{inc} &\propto \cos(\alpha) \\ E_{\hat{v}}^{inc} &\propto \sin(\alpha) \end{aligned} \quad (3).$$

where α is the bearing angle of the UAV, i.e. the horizontal rotation measured counterclockwise from the East direction (see illustration in Fig. 3). Combining (1), (2) and (3), the following relations for the voltage output of the two polarimeter channels can be obtained:

$$\begin{aligned} v_a &\propto \cos(\delta_a)\cos(\alpha) + \sin(\delta_a)e^{j\varphi_a}\sin(\alpha) \\ v_b &\propto m_{ab}e^{j\varphi_{ab}}(-\sin(\delta_b)\cos(\alpha)\,e^{j\varphi_b} + \cos(\delta_b)\sin(\alpha)) \end{aligned} \quad (4).$$

The parameters required for the IXR computation i.e. δ_a, φ_a, δ_b, φ_b and m_{ab} are obtained from the polarimeter response (5) through a best-fitting procedure with

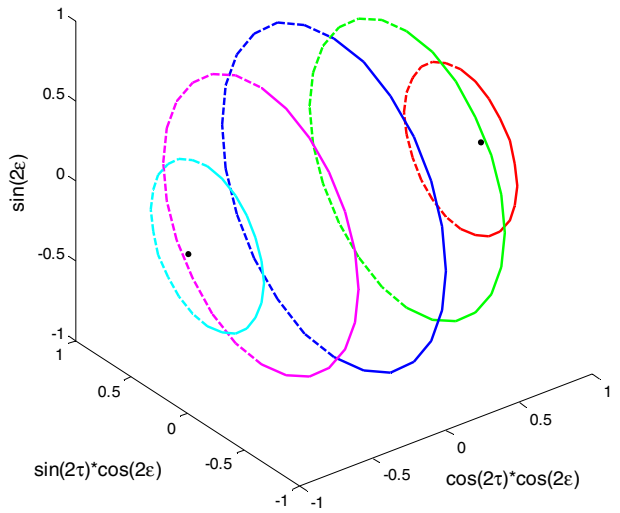

Figure 2. Representation on the Poincaré sphere obtained from the parametrization in (2). Colored circles for constant values of $|\delta|$ and 180° variation of φ. Solid/dashed lines for positive/negative δ. Black markers for $\delta = 0°$ (left) and $|\delta| = 90°$ (right).

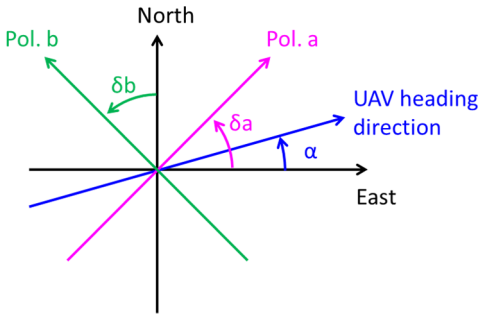

Figure 3. Illustration of the parameters δ_a (magenta), δ_b (green) and the UAV bearing angle α (blue) in a Cartesian reference system.

parametrized curves. In the next section, an experimental result obtained on a station of the LOFAR radio telescope is discussed.

3. Experimental Result on LOFAR

LOFAR consists of several stations spread over Europe, each of them composed of two subarrays: a Low Band Antenna (LBA) array and a High Band Antenna (HBA) array, covering the frequency range 10–90 MHz and 120–240 MHz, respectively.
The LBA consists of two orthogonal inverted-V dipoles above a ground plane [14]. The two antenna polarizations are nominally oriented along the North-East (NE) direction and the North-West (NW) one. With reference to Fig. 3, $\delta_a^{nom} = \delta_b^{nom} = 45°$ (nominal values).
A spin flight above the center of the LBA array has been performed. In this configuration, the UAV slowly rotates around the vertical axis i.e. the bearing angle α is varied (see Fig. 3), while aiming to keep a fixed position at the zenith ($\vartheta = 0°$) of the central element of the LBA array (LBA antenna #0). Fig. 4a shows the UAV bearing angle

vs. time, acquired by the onboard Inertial Measurement Unit (IMU) whereas Fig. 4b shows the observation angle with respect to the zenith direction (ϑ coordinate of the UAV), computed from the Differential GNSS position data [11].

The amplitude response for both LBA #0 polarizations is shown in Fig. 5 as a function of UAV bearing angle (magenta and green curves). The working frequency is 57 MHz. Both curves have been normalized with respect to their maximum value. The difference between the normalization values, corresponding to m_{ab} in (3), is within 0.1 dB. This difference yields IXR levels higher than 40 dB, which can be considered as negligible with respect to the contributions discussed below.

The plot in Fig. 5 also shows, for each polarization, the best-fitting curves (blue and red) that allow to quantify the angular parameters δ_a, φ_a, δ_b and φ_b, of interest for the IXR estimation. The best-fit φ_a and φ_b values are basically 0°. This is consistent with the deep nulls in Fig. 5. The measured angular positions of the minima (best-fit curves) are $\delta_a = 40.3°$ and $\delta_b = 41.8°$.

An angular offset of the minima for both polarizations is apparent, i.e. $e_a = \delta_a - \delta_a^{nom} = -4.7°$ (NE pol.) and $e_a = \delta_a - \delta_a^{nom} = -3.2°$ (NW pol.). The average of these two errors reveals a rotation offset between the measured polarization directions and the expected ones. The orientation of the LBA polarizations have been experimentally verified by means of topographic tools (total station). The measured rotations with respect to the nominal values were within 0.2°. Therefore, the aforementioned rotation offset is basically due to the magnetometer calibration error in the UAV.

Nevertheless, the relevant quantity as far as the IXR measurement is concerned is the difference between δ_a and δ_b. This affects the condition number of the matrix in (2). Their difference, i.e. $\delta_a - \delta_b = -1.5°$, gives an IXR better than 35 dB at zenith.

It should be pointed out that this small angular value is comparable to the accuracy of the IMU on board the UAV (about 2°). Therefore, the estimated IXR level of 35 dB can be considered as the limit of the present measurement system implementation. This is already useful in the context of SKA1-LOW development, where the IXR requirements are in the order of 15 dB [15]. Other techniques, such as laser tracking, could provide superior accuracy in the measurement of the UAV orientation, at a higher cost.

4. Conclusion

A UAV-based measurement procedure for the estimation of the IXR has been experimentally applied on a station of the LOFAR radio telescope at the working frequency of 57 MHz, obtaining valuable preliminary results. The estimated accuracy is consistent with the IXR characterization requirements of phased arrays for radio astronomy. A more extended validation work for the presented procedure is ongoing.

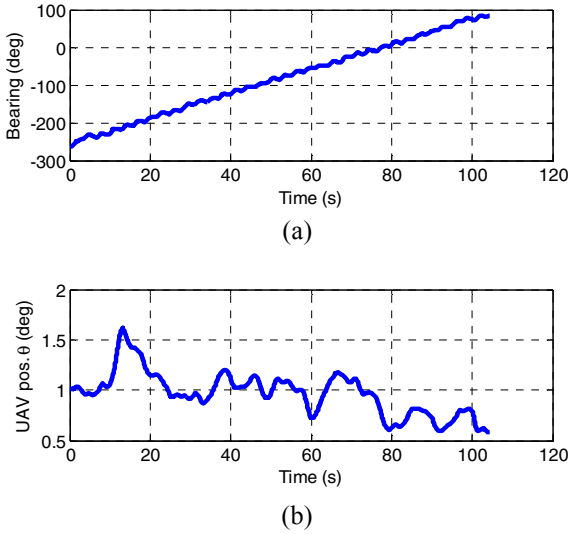

Figure 4. (a) UAV bearing angle during the measurement. (b) UAV position (ϑ coordinate) in the array-centered reference system.

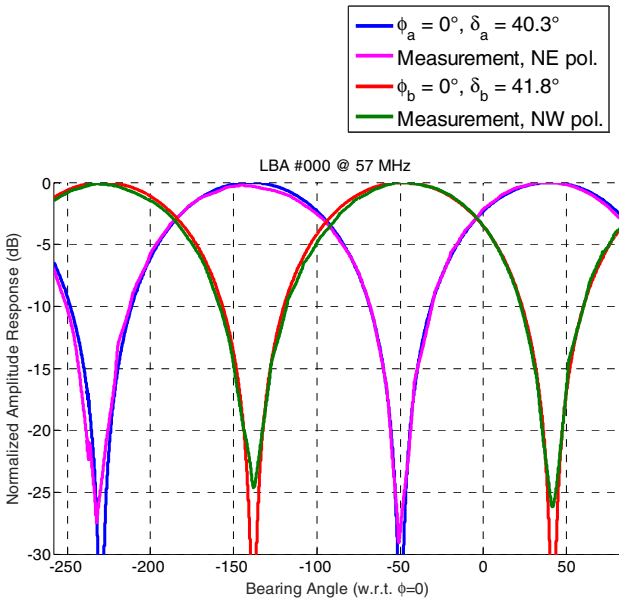

Figure 5. Normalized amplitude response for the spin flight at the zenith of the LBA array. Measurement, NE pol. (magenta); measurement, NW pol. (green); best fitting curve, NE pol. (blue); best fitting curve, NW pol. (red).

5. Acknowledgements

The authors thank Menno Norden from ASTRON, Paolo Maschio from Politecnico di Torino (DIATI), and Augusto Olivieri from CNR-IEIIT for their valuable technical contribution to the experimental activity.

6. References

[1] T. D. Carozzi and G. Woan, "A Fundamental Figure of Merit for Radio Polarimeters," *IEEE Trans. Antennas Propag.*, vol. 59, no. 6, pp. 2058-2065, June 2011. doi: 10.1109/TAP.2011.2123862.

[2] S. J. Wijnholds, M. V. Ivashina, R. Maaskant and K. F. Warnick, "Polarimetry With Phased Array Antennas: Sensitivity and Polarimetric Performance Using Unpolarized Sources for Calibration," *IEEE Trans. Antennas Propag.*, vol. 60, no. 10, pp. 4688-4698, Oct. 2012. doi: 10.1109/TAP.2012.2207340.

[3] B. Fiorelli, M. Arts, G. Virone, E. de Lera Acedo and W. A. van Cappellen, "Polarization analysis and evaluation for radio astronomy aperture array antennas," *2013 7th European Conference on Antennas and Propagation (EuCAP)*, Gothenburg, 2013, pp. 461-465.

[4] B. Fiorelli, E. de Lera Acedo, M. Arts, G. Virone and J. G. bij de Vaate, "Polarization performances and antenna misalignment errors for aperture arrays: SKA-low AAVS0.5 case," *2013 International Conference on Electromagnetics in Advanced Applications (ICEAA)*, Torino, 2013, pp. 972-975. doi: 10.1109/ICEAA.2013.6632385.

[5] B. Fiorelli and E. De Lera Acedo, "On the simulation and validation of the Intrinsic Cross-Polarization Ratio for antenna arrays devoted to low frequency radio astronomy," *The 8th European Conference on Antennas and Propagation (EuCAP 2014)*, The Hague, 2014, pp. 2361-2364. doi: 10.1109/EuCAP.2014.6902290.

[6] A. T. Sutinjo and P. J. Hall, "Intrinsic Cross-Polarization Ratio of Dual-Linearly Polarized Antennas for Low-Frequency Radio Astronomy," *IEEE Trans. Antennas Propag.*, vol. 61, no. 5, pp. 2852-2856, May 2013. doi: 10.1109/TAP.2013.2243101.

[7] J. G. bij de Vaate, P. Benthem, and H. Schnetler, "The SKA low frequency aperture array", *Proc. SPIE 9908, Ground-based and Airborne Instrumentation for Astronomy VI*, 99083X (9 August 2016); doi: 10.1117/12.2231618.

[8] G. Virone et al., "UAV-based technique for the characterization of the Intrinsic Cross-Polarization Ratio (IXR)," *2017 11th European Conference on Antennas and Propagation (EUCAP)*, Paris, 2017, pp. 3825-3828. doi: 10.23919/EuCAP.2017.7928714.

[9] G. Virone et al., "Antenna Pattern Verification System Based on a Micro Unmanned Aerial Vehicle (UAV)," *IEEE Antennas Wireless Propag. Lett.*, vol. 13, pp. 169-172, 2014. doi: 10.1109/LAWP.2014.2298250.

[10] P. Bolli et al., "From MAD to SAD: the Italian experience for the Low Frequency Aperture Array of SKA1-LOW," *Radio Science*, vol. 51, issue 3, pp. 160–175, Mar. 2016.

[11] G. Pupillo et al., "Medicina Array Demonstrator: calibration and radiation pattern characterization using a UAV-mounted radio-frequency source," *Experimental Astronomy*, vol. 39, issue 2, pp. 405-421, June 2015.

[12] E. de Lera Acedo et al., "SKA aperture array verification system: electromagnetic modeling and beam pattern measurements using a micro UAV," *Experimental Astronomy*, 2017. doi: https://doi.org/10.1007/s10686-017-9566-x. In Press.

[13] F. Paonessa et al., "Recent results on the characterization of the LOFAR radio telescope by means of a micro UAV," *2017 International Conference on Electromagnetics in Advanced Applications (ICEAA)*, Verona, 2017, pp. 1752-1753. doi: 10.1109/ICEAA.2017.8065634.

[14] M. P. van Haarlem et al., "LOFAR: The Low-Frequency ARray," *Astronomy & Astrophysics*, vol. 556, 2013. doi: https://doi.org/10.1051/0004-6361/201220873.

[15] M. G. Labate, L. Stringhetti, M. Waterson, J. Wagg, R. Braun, P. Dewdney, P. Gibbs, "SKA1-Low Antenna Evaluation Criteria," SKA-TEL-SKO-0000800, rev. 1, 2017-08-30.